TSC1 intragenic deletion transmitted from a mosaic father to two siblings with cardiac rhabdomyomas: identification of two aberrant transcripts

TSC1 intragenic deletion transmitted from a mosaic father to two siblings with cardiac rhabdomyomas: identification of two aberrant transcripts

Hiroki Uchiyama[a]*, Yohei Masunaga[a]*, Takamichi Ishikawa[a], Tetsuya Fukuoka[b], Maki Fukami[c], Hirotomo Saitsu[d], Tsutomu Ogata[a]†

[a] *Department of Pediatrics, Hamamatsu University School of Medicine, Hamamatsu, Japan*

[b] *Department of Pediatrics, Shizuoka Saiseikai General Hospital, Shizuoka, Japan*

[c] *Department of Molecular Endocrinology, National Research Institute for Child Health and Development, Tokyo, Japan*

[d] *Department of Biochemistry, Hamamatsu University School of Medicine, Hamamatsu, Japan*

*Contributed equally to this work.

†Correspondence to: Tsutomu Ogata, Department of Pediatrics, Hamamatsu University School of Medicine, Hamamatsu 431-3192, Japan. E-mail: tomogata@hama-med.ac.jp

Abstract

Tuberous sclerosis complex (TSC) is a rare autosomal dominant disorder characterized by non-cancerous tumors in multiple organs including the brain, kidney, lung, heart, and skin. We encountered a Japanese family consisting of two siblings (a four-year-old boy and a one-year-old girl) with multiple cardiac rhabdomyomas conveying a high risk of TSC and apparently unaffected sibling (a two-year-old girl) and parents. Whole exome sequencing and application of Integrative Genomic Viewer revealed an identical intragenic *TSC1* deletion with the breakpoints on intron 15 and exon 19 in the affected siblings, but not in the apparently unaffected sibling and parents. Subsequently, PCR-based analyses were performed using primers flanking the deletion, showing that the deletion was also present in the father and that the deletion occurred between chr9:135,777,038 (bp) and chr9:135,780,540 (bp) in association with a one bp overlap. Furthermore, RT-PCR analyses were carried out using lymphoblastoid cell lines, revealing a major in-frame insertion/deletion transcript produced by aberrant splicing using a cryptic ″ag″ splice acceptor motif at intron 15 (r.1998_2438delinsTTCATTAGGTGG) and a minor frameshift transcript generated by aberrant splicing between exon 15 and exon 20 (r.1998_2502del, p.Lys666Asnfs*15) in the affected siblings. These findings imply that the intragenic deletion producing two aberrant transcripts was generated as a somatic pathogenic variant involving the germline in the father and was transmitted to the affected siblings.

Keywords: *TSC1*, tuberous sclerosis complex, cardiac rhabdomyoma, germline mosaicism, intragenic deletion, aberrant transcript

Introduction

Tuberous sclerosis complex (TSC) is a rare autosomal dominant disorder characterized by non-cancerous tumors in multiple organs including the brain, kidney, lung, heart, eyes, liver, and skin (Curatolo et al., 2008). Developmental delay and seizure are also observed frequently. The prevalence is ~ one in 6,000 to 10,000 subjects, and ~ two-thirds of patients are identified as sporadic cases born to apparently healthy parents (Curatolo et al., 2008; Peron et al., 2018). TSC is caused by pathogenic variants of either *TSC1* encoding hamartin or *TSC2* encoding tuberin. Hamartin and tuberin act as tumor suppressors, and the hamartin-tuberin complex regulates cell growth and division by suppressing the function of the mammalian target of rapamycin complex 1 (mTORC1) (Curatolo et al., 2008). Thus, pathogenic variants of *TSC1* or *TSC2* result in the tumor development because of the activation of the mTORC1 function. Furthermore, since a second event including loss of heterozygosity is frequently found in tumor tissues (Rosset et al., 2017), it is likely that biallelic pathogenic variants of *TSC1*/*TSC2* lead to the development of non-cancerous tumors.

Here, we report two Japanese siblings with cardiac tumors as the sole recognizable abnormality and a *TSC1* intragenic deletion producing two aberrant transcripts which was inherited from their clinically unaffected mosaic father.

Clinical report

We encountered a Japanese family with two siblings who received the possible diagnosis of TSC because of the presence of multiple cardiac rhabdomyomas. The male proband (case II-1 in Figure 1A) was noticed to have cardiac tumors by fetal ultrasonography at 31 weeks of gestation. He was born at 37 weeks of gestation by vaginal delivery without neonatal asphyxia. At birth, his length was 47.5 cm (~ 50 percentile), and his weight 2947 g (50–75 percentile). Physical examination at birth showed no abnormalities including the skin, although a wood lamp examination was not performed (Yates, 2006). Postnatal echocardiography confirmed multiple cardiac tumors of 6.3–15.8 mm in diameter in right ventricle (RV) and left ventricle (LV). Hemodynamics remained stable without ventricular inflow or outflow obstruction by the tumors. Electrocardiogram (ECG) was normal. Since the

tumors were suspected as rhabdomyomas characteristic of TSC (Rosset et al., 2017), we performed brain magnetic resonance imaging (MRI), ophthalmologic examinations, and visceral ultrasound studies, detecting no other features reported in TSC (Krueger and Northrup, 2013). Echocardiography was performed at a ~ two months interval, showing spontaneous regression of the tumors, as has been reported for rhabdomyomas in TSC (Curatolo et al., 2008). On the last examination at four years of age, while he still had small cardiac tumors, he showed apparently normal growth and development with no episode of seizures.

The third female child (case II-3 in Figure 1A) was also found to have cardiac tumors by echocardiography performed shortly after birth because of the history of cardiac tumors in case II-1. She was born at 32 weeks of gestation, with a birth length of 43.0 cm (50–75 percentile) and a birth weight of 1,820 g (50 percentile). Her cardiac tumors were 6.2–15.2 mm in diameter and were identified at multiple locations including the RV free wall to interventricular septum, RV apex, LV free wall to interventricular septum, and the vicinity of anterior papillary muscle of LV (Figure 1B). There was no ventricular inflow or outflow obstruction. ECG was normal. Physical examination at birth was non-remarkable including the skin, although a wood lamp examination was not performed (Yates, 2006). She was also suspected to have cardiac rhabdomyomas characteristic of TSC, but brain MRI, ophthalmologic examinations, and visceral ultrasound studies showed no other abnormal findings described in TSC (Krueger and Northrup, 2013). The cardiac tumors gradually diminished in size. On the last examination at one year of age, she remained healthy with normal growth and development.

The two-year-old second child (case II-2 in Figure 1A) had no clinically discernible TSC features including cardiac masses on echocardiograms. The non-consanguineous parents had no history of cardiac, renal, brain, and skin diseases.

After the genetic diagnosis, we planned to perform electroencephalographic studies and the TSC-Associated-Neuropsychiatric-Disorders evaluation in the affected siblings before entering a junior school, as has been recommended (Krueger and Norturup, 2013). Although we suggested to the father to receive detailed examinations for TSC features, he refused such

examinations primarily because of lack of clinical symptoms. Thus, it was unknown whether the father had cryptic clinical features of TSC.

Methods

This study was approved by the Institutional Review Board Committee at Hamamatsu University School of Medicine, and was performed after obtaining written informed consent. We performed whole exome sequencing (WES) using leukocyte genomic DNA (gDNA) samples, to examine two possibilities: (1) the siblings had a monoallelic dominant pathogenic variant in *TSC1* or *TSC2* that was transmitted from either of the parents with germline mosaicism or intra-familial clinical variability, and (2) they had biallelic recessive pathogenic variants in a hitherto unknown gene for cardiac tumors. WES was carried out with SureSelect Human All Exon V6 (Agilent Technologies), and captured libraries were sequenced by NextSeq 500 (Illumina) with 150 bp paired-end reads. Reads were aligned to the reference genome (Human GRCh37/hg19) (UCSC Genome Browser; http://genome.ucsc.edu/) using BWA-MEM (Version 0.7.12) with default parameters. Data processing, variant calling, annotation, and filtering were performed as previously described (Miyado et al., 2019). Final variants were annotated with Annovar (Wang et al., 2010).

To examine the structure of transcripts and the occurrence of nonsense mediated mRNA decay (NMD) (Kuzmiak and Maquat, 2006), we performed reverse-transcriptase (RT)-PCR for mRNAs extracted from lymphoblastoid cell lines (LCLs) incubated for 8 hours with NMD inhibitor cycloheximide (CHX) (Sigma) or with dimethyl sulfoxide as a control material. Subsequently, RT-PCR products were subjected to electrophoresis and direct sequencing.

Results

WES was performed for the affected siblings (II-1 and II-3) and the parents, identifying apparently *de novo* sequence variants at exon 19 of *TSC1* which were initially evaluated as three successive 4–6 bp insertions, *i.e.*, c.2433_2434insTATC, c.2437_2438insTTCATT, and c.2438_2439insGGTGG, in both the affected siblings (reference sequence: *TSC1* transcript variant 1, Genbank NM_000368.4) (http://www.ncbi.nlm.nih.gov/). Since such a complicated

finding indicated genomic alteration affecting exon 19 of *TSC1*, we performed manual inspection of aligned sequences around exon 19 by Integrative Genomic Viewer (IVG) (https://www.igv.org). Consequently, clipped and discordant read pairs which aligned to the sequence of exon 19 and that of intron 15 were identified in the affected siblings, whereas such aberrant reads were undetected in the parents (Figure 2A). Furthermore, genotyping for rs75802666 revealed that the siblings were heterozygous for the paternally inherited ″T″ allele and maternally derived ″C″ allele, and that the clipped and discordant reads were associated with the ″T″ allele. These findings indicated the presence of an identical deletion spanning from 3′-region of intron 15 to 5′-region of exon 19 on the paternally inherited *TSC1* of the affected siblings. We next performed PCR amplification with primers flanking the deletion and those for non-deleted wildtype allele, detecting the deletion in the father as well as in the affected siblings, but not in the mother and the unaffected sibling (II-2) (Figure 2B). This showed that the deletion took place as a somatic mosaicism involving germline in the father. In addition, Sanger sequencing of the PCR products showed that the deletion occurred between chr9:135,777,038 (bp) and chr9:135,780,540 (bp) in association with a one bp overlap, and that the sequence of intron 15 contained the three 4–6 bp segments incorrectly evaluated as insertions. Assuming that the overlapping one bp is g.135,777,039 (bp) at exon 19, this deletion is described as NC_000009.11:g.135777040_135780539del (NM_000368.4:c.1997+429_2438del). The breakpoints were found to reside on non-repeat sequences by Repeatmasker (http://www.repeatmasker.org). This intragenic deletion was absent from gnomAD database (http://gnomad.broadinstitute.org/), Human Genetic Variation database (http://www.hgvd.genome.med.kyoto-u.ac.jp/), and allele frequency data of ,4773 Japanese individuals (4.7KJPN) (https://jmorp.megabank.tohoku.ac.jp/). We deposited this deletion in the Leiden Open Variation Database (LOVD) (http://databases.lovd.nl/shared/genes) (ID: 0000674869).

We further searched for other variant(s) which satisfied the following criteria: (1) segregation pattern consistent with Mendelian inheritance with complete penetrance; (2) minor allele frequency of ≤ 0.01 in the above three public databases; and (3) high pathogenicity predicted by Combined Annotation-Dependent Depletion

(http://cadd.gs.washington.edu/snv) and Polyphen-2_HumVar (http://genetics.bwh.harvard.edu/pph2/). However, there was no such a variant in this family.

We next performed RT-PCR with primers for exon 15 and exon 20, revealing two aberrant mRNAs (transcript-1 and transcript-2) and wildtype mRNA in the affected siblings, and wildtype mRNA alone in the parents and the unaffected sibling (Figure 3A). The bands for transcript-1 were clearly identified with and without CHX treatment, whereas those for transcript-2 were quite faint without CHX treatment and weakly detected with CHX treatment. This indicated that transcript-1 escaped NMD, whereas transcript-2 grossly underwent NMD. Sequencing analysis showed that transcript-1 was produced by aberrant splicing using a cryptic ″ag″ splice acceptor motif at intron 15 (r.1998_2438delinsTTCATTAGGTGG) (Figure 3B). Indeed, the cryptic splice acceptor motif was found to be accompanied by a pyrimidine (Y)-rich sequence and a candidate branch site required for splicing (Strachan and Read, 2011) by SVM-BP finder (http://regulatorygenomics.upf.edu/Software/SVM_BP). Since transcript-1 was associated with in-frame insertion and deletion, this was consistent with transcript-1 escaping NMD. Sequencing analysis also revealed that transcript-2 was generated by aberrant splicing between exon 15 and exon 20 (r.1998_2502del, p.Lys666Asnfs*15) (Figure 3C). Since transcript-2 harbored a premature stop codon on exon 20 because of the frameshift, this was compatible with transcript-2 being subject to NMD.

Discussion

Molecular studies identified a heterozygous intragenic deletion of *TSC1* in two Japanese siblings with cardiac rhabdomyomas. Unpredictably, RT-PCR analyses revealed a major transcript-1 produced with a cryptic splice acceptor motif at intron 15, as well as a minor transcript-2 generated with a wildtype splice acceptor motif at intron 19. Both transcript-1 and transcript-2 were missing 5′-region of the coiled coil domain and tuberin interaction domain (Peron et al., 2018), and transcript-2 was primarily subject to NMD. According to the ACMG Standards and Guidelines (Richards et al., 2015), the intragenic deletion (NC_000009.11:g.135777040_135780539del) is regarded as "pathogenic", because they are

positive for PVS1 (multiexon deletion), PS3 (confirmation by RNA analysis), PM2 (absence from controls), and PP4 (patient′s phenotype specific for a disease with a single genetic etiology). In addition, since this deletion occurred between non-homologous regions and was mediated by one bp microhomology, it is likely that the deletion was generated by replication-based mechanisms such as fork stalling and template switching and microhomology-mediated break-induced replication (Nilsson et al., 2017). To our knowledge, this intragenic deletion has not been reported, although a number of variants including a similar intragenic deletion involving *TSC1* exons 15–19 has been registered in the LOVD database.

Genetic studies were useful to confirm the diagnosis of TSC. In this regard, targeted *TSC1*/*TSC2* sequencing by next generation sequencer (NGS) (or classic Sanger method), followed by deletion/duplication analysis for the two genes by several methods (*e.g.*, quantitative PCR, multiplex ligation-dependent probe amplification, and array comparative hybridization) in the absence of a sequence variant, has been regarded as the gold standard genetic test for TSC, and a multigene NGS panel and WES are considered when clinical features are mild or obscure (Peron et al., 2018). This current genetic approach is rational and useful. Indeed, the intragenic deletion identified in this study would be detected by deletion/duplication analysis. However, WES can identify sequence variants not only in previously known genes but also in hitherto unknown genes. Furthermore, because of the development of applications, WES can reveal sequence disruption by employing IGV (as shown here), various sizes of deletions/duplications by utilizing WES-based copy-number variant calling (Nord et al., 2011) and eXome Hidden Markov Model (Fromer and Purcell, 2014), and full or segmental disomies by estimating B-allele frequencies for single nucleotide polymorphisms (Yauy et al., 2020). Considering such increasing utility and improved cost-performance, we performed WES from the outset in this study.

The affected siblings had cardiac rhabdomyomas as the sole recognizable abnormality. This may be due to the young ages of the siblings (four years and one year), because *TSC1* pathogenic variants are associated with multiple features in an age-dependent manner. For example, TSC is associated with cardiac rhabdomyomas in 30–50% of patients from the late fetal period to early infancy, intellectual disability in 30–50% of patients from infancy,

epilepsy in 60–70% of patients from infancy, retinal hamartomas in ~50% of patients from infancy, hypomelanotic macules in ~90% of patients from infancy to childhood, facial angiofibromas in ~75% of patients from childhood, and renal angiomyolipomas in ~80% of patients from childhood to puberty (Northrup and Krueger, 2013; Curatolo et al., 2008; Rosset et al., 2017; Wataya-Kaneda et al., 2013). Thus, the siblings may exhibit additional major and/or minor clinical features of TSC in later ages. Importantly, since cardiac rhabdomyoma is regarded as an indication for possible TSC (Northrup and Krueger, 2013), it is recommended to perform genetic diagnosis and clinical workup in patients with cardiac rhabdomyoma (Krueger and Northrup, 2013).

The father was found to have somatic mosaicism involving germline, although we could not examine the frequency of *TSC1* mosaicism in his sperms. In this regard, two matters are notable. First, germline mosaicism may be not so rare in TSC. Indeed, several families harboring ≥ two affected children born to apparently unaffected parents have been reported (Rose et al., 1999). Furthermore, because of the possibility of latent mosaicism, the recurrent risk has been estimated to be up to 2% in families with apparently sporadic TSC (Peron et al., 2018). Second, even individuals with low-level (<10%) mosaicism almost invariably have ≥ two TSC clinical features especially facial angiofibromas and renal angiomyolipomas, although the phenotypic severity remain milder than that of non-mosaic patients (Giannikou et al., 2019). Thus, it is possible that some clinical feature remained undetected in the father and/or that he had some clinical feature such as cardiac rhabdomyomas at a younger age.

In summary, we identified *TSC1* intragenic deletion producing two aberrant transcripts which was transmitted from mosaic father to two siblings with cardiac rhabdomyomas. The results argue for the value of molecular studies in the identification of underlying genetic cause.

Declaration of competing interest

The authors declare no conflict of interest.

Acknowledgments

We thank Ms. Fumiko Kato, Ms. Aya Kitamoto, Mr. Naoki Adachi, and Mr. Ryo Horiguchi for their technical support.

Funding sources

This work was supported by Grants from the Japan Agency for Medical Research and Development (AMED) (JP19ek0109301 and JP19ek0109297).

References

Curatolo, P., Bombardieri, R., Jozwiak, S., 2008. Tuberous sclerosis. Lancet. 372, 657-668. https://doi.org/10.1016/S0140-6736(08)61279-9.

Fromer, M., Purcell, S.M., 2014. Using XHMM software to detect copy number variation in whole-exome sequencing data. Curr. Protoc. Hum. Genet. 81, 7.23.1-21. http://doi.org/10.1002/0471142905.hg0723s81.

Giannikou, K., Lasseter, K.D., Grevelink, J.M., Tyburczy, M.E., Dies, K.A., Zhu, Z., Hamieh, L., Wollison, B.M., Thorner, A.R., Ruoss, S.J., Thiele, E.A., Sahin, M., Kwiatkowski, D.J., 2019. Low-level mosaicism in tuberous sclerosis complex: prevalence, clinical features, and risk of disease transmission. Genet. Med. 21, 2639-2643. https://doi.org/10.1038/s41436-019-0562-6.

Krueger, D.A., Northrup, H., 2013. Tuberous sclerosis complex surveillance and management: Recommendations of the 2012 international tuberous sclerosis complex consensus conference. Pediatr. Neurol. 49, 255-265. https://doi.org/10.1016/j.pediatrneurol.2013.08.002.

Kuzmiak, H.A., Maquat, L.E., 2006. Applying nonsense-mediated mRNA decay research to the clinic: progress and challenges. Trends. Mol. Med. 12, 306–316. https://doi.org/10.1016/j.molmed.2006.05.005.

Miyado ,M., Fukami, M., Takada, S., Terao, M., Nakabayashi, K., Hata, K., Matsubara, Y., Tanaka, Y., Sasaki, G., Nagasaki, K., Shiina, M., Ogata, K., Masunaga, Y., Saitsu, H., Ogata, T., 2019. Germline-derived gain-of-function variants of Gsα-coding *GNAS* gene identified in nephrogenic syndrome of inappropriate antidiuresis. J. Am. Soc. Nephrol. 30, 877–889. https://dx.doi.org/10.1681%2FASN.2018121268.

Nilsson, D., Pettersson, M., Gustavsson, P., Förster, A., Hofmeister, W., Wincent, J., Zachariadis, V., Anderlid, B.M., Nordgen, A., Mäkitie, O., Wirta, V., Käller, M., Vezzi, F., Lupski, J.R., Nordenskjöld, M., Lundberg, E.S., Carvalho, C.M.B., Lindstrand, A., 2017. Whole-genome sequencing of cytogenetically balanced chromosome translocations identifies potentially pathological gene disruptions and highlights the importance of

279 microhomology in the mechanism of formation. Hum. Mutat. 38, 180–192.
280 https://doi.org/10.1016/j.molmed.2006.05.005.
281 Nord, A.S., Lee, M., King, M.C., Walsh, T., 2011. Accurate and exact CNV identification
282 from targeted high-throughput sequence data. BMC. Genomics. 12:184.
283 https://doi.org/10.1186/1471-2164-12-184.
284 Northrup, H., Krueger, D.A., 2013. Tuberous sclerosis complex diagnostic criteria update:
285 Recommendations of the 2012 international tuberous sclerosis complex consensus
286 conference. Pediatr. Neurol. 49, 243-254.
287 http://doi.org/10.1016/j.pediatrneurol.2013.08.001.
288 Peron, A., Au, K.S., Northrup, H., 2018. Genetics, genomics, and genotype-phenotype
289 correlations of TSC: Insights for clinical practice. Am. J. Med. Genet. 178, 281-290.
290 https://doi.org/10.1002/ajmg.c.31651.
291 Richards, S., Aziz, N., Bale, S., Bick, D., Das, S., Gastier-Foster, J., Grody, W.W., Hegde,
292 M., Lyon, E., Spector, E., Voelkerding, K., Rehm, H.L., ACMG Laboratory Quality
293 Assurance Committee, 2015. Standards and guidelines for the interpretation of
294 sequence variants: a joint consensus recommendation of the American College of
295 Medical Genetics and Genomics and the Association for Molecular Pathology. Genet.
296 Med. 17, 405-424. http://doi.org/10.1038/gim.2015.30.
297 Rose, V.M., Au, K.S., Pollom, G., Roach, E.S., Prashner, H.R., Northrup, H., 1999. Germ-
298 line mosaicism in tuberous sclerosis: How common? Am. J. Hum. Genet. 64, 986-992.
299 https://doi.org/10.1086/302322.
300 Rosset, C., Netto, C.B.O., Ashton-Prolla, P., 2017. TSC1 and TSC2 gene mutations and their
301 implications for treatment in tuberous sclerosis complex: a review. Genet. Mol. Biol.
302 40, 69-79. http://dx.doi.org/10.1590/1678-4685-GMB-2015-0321.
303 Strachan, T., Read, A.P., 2011. Nucleic acid structure and gene expression, In: Strachan, T.,
304 Read, A.P. (Eds.), Human molecular genetics, fourth ed., New York: Garland Science,
305 pp. 1-27.

306 Wang, K., Li, M., Hakonarson, H., 2010. ANNOVAR: functional annotation of genetic
307 variants from high-throughput sequencing data. Nucleic. Acids. Res. 38, e164.
308 https://doi.org/10.1093/nar/gkq603.
309 Wataya-Kaneda, M., Tanaka, M., Hamasaki, T., Katayama, I., 2013. Trends in the prevalence
310 of tuberous sclerosis complex manifestations: An epidemiological study of 166 Japanese
311 patients. PLoS. One. 8, e63910. https://doi.org/10.1371/journal.pone.0063910.
312 Yates, J.R.W., 2006. Tuberous sclerosis. Eur. J. Hum. Genet. 14, 1065-1073.
313 https://doi.org/10.1038/sj.ejhg.5201625.
314 Yauy, K., Leeuw, N., Yntema, H.G., Pfundt, R., Gilissen, C., 2020. Accurate detection of
315 clinically relevant uniparental disomy from exome sequencing data. Genet. Med. 22, 803-
316 808. https://doi.org/10.1038/s41436- 019-0704-x.
317

Figure Legends

Figure 1. Clinical findings.

A. The pedigree of this family.

B. Echocardiographic images of case II-3 (left, parasternal short axis view; and right, apical 4-chamber view). RV, right ventricle; LV, left ventricle; APM, anterior papillary muscle; PPM, posterior papillary muscle; RA, right atrium; and LA, left atrium.

Figure 2. Summary of molecular studies using gDNA.

A. IVG screen-shot of WES pair-end reads.

B. PCR-based analyses of the deletions. *TSC1* consists of 23 exons and encodes 1,164 amino acids. P1–P3 indicate the genomic positions of the utilized primers (P1, 5′-TGTGTAGCCTCAGGGCTCTT-3′; P2, 5′-GGCCATTTTATGCCTCTGTT-3′; and P3, 5′-GATACCAGCAGCACCAAAAAC-3′).

Figure 3. Summary of molecular studies using mRNA.

A. RT-PCR products obtained with P4 and P5 primers (P4, 5′-CCAAAGCAAGCCTTTACTCC-3′; and P5, 5′-TGAGTGCTTGTTCTGCAGTTG-3′).

B. Genomic sequence around the fusion point between retained intron 15 and exon 19 and partial electrochromatogram of transcript-1, indicating aberrant splicing using an alternative ″ag″ splice acceptor motif accompanied by a pyrimidine (Y)-rich sequence and a putative branch site at intron 15; the "a" nucleotide highlighted with red at the putative branch site is highly conserved among branch sites. On the electrochromatogram, exonic and transcribed intronic nucleotides are written with large and small letters, respectively; the ″A″ nucleotide highlighted with yellow is provisionally assigned to exon 19, although it is shared by intron 15 and exon 19 (see Figure 2B).

C. Partial electrochromatogram of transcript-2, showing aberrant splicing between exon 15 and exon 20.

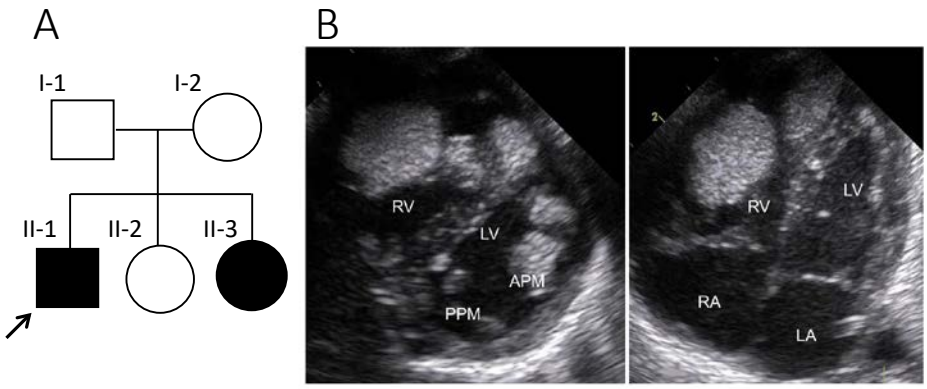
A
I-1
I-2
II-1
II-2
II-3
B
RV
LV
APM
PPM
RV
LV
RA
LA

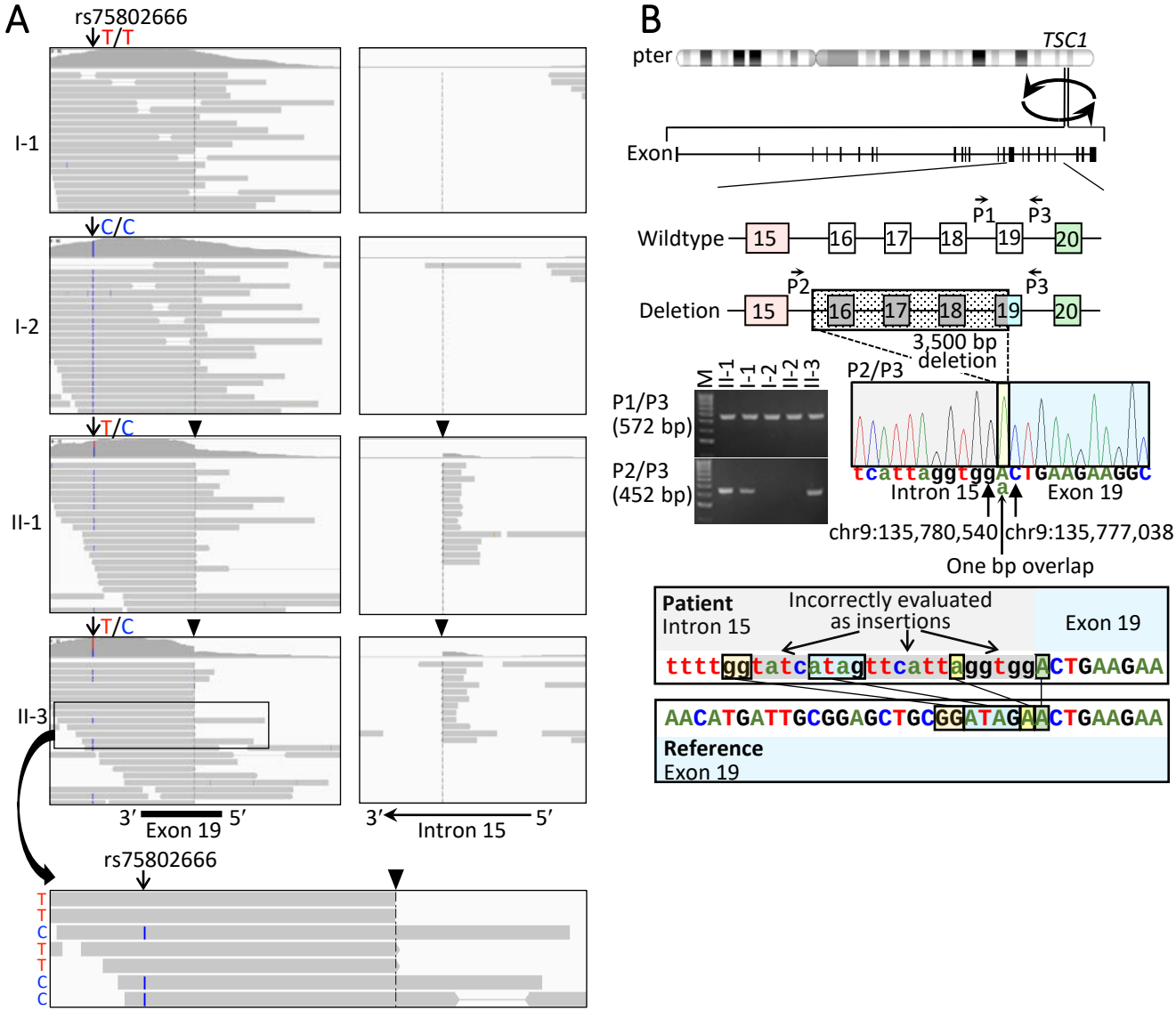
A
rs75802666
T/T
I-1
C/C
I-2
T/C
II-1
T/C
II-3
3′
Exon 19
5′
3′
Intron 15
5′
rs75802666
T
T
C
T
T
C
C
B
pter
TSC1
Exon
Wildtype
15
16
17
18
19
20
P1
P3
Deletion
P2
P3
3,500 bp
deletion
M
II-1
I-1
I-2
II-2
II-3
P1/P3
(572 bp)
P2/P3
(452 bp)
P2/P3
tcattaggtggACTGAAGAAGGC
Intron 15
a
Exon 19
chr9:135,780,540
chr9:135,777,038
One bp overlap
Patient
Intron 15
Incorrectly evaluated
as insertions
Exon 19
ttttggtatcatagttcattaggtggACTGAAGAA
AACATGATTGCGGAGCTGCGGATAGAACTGAAGAA
Reference
Exon 19

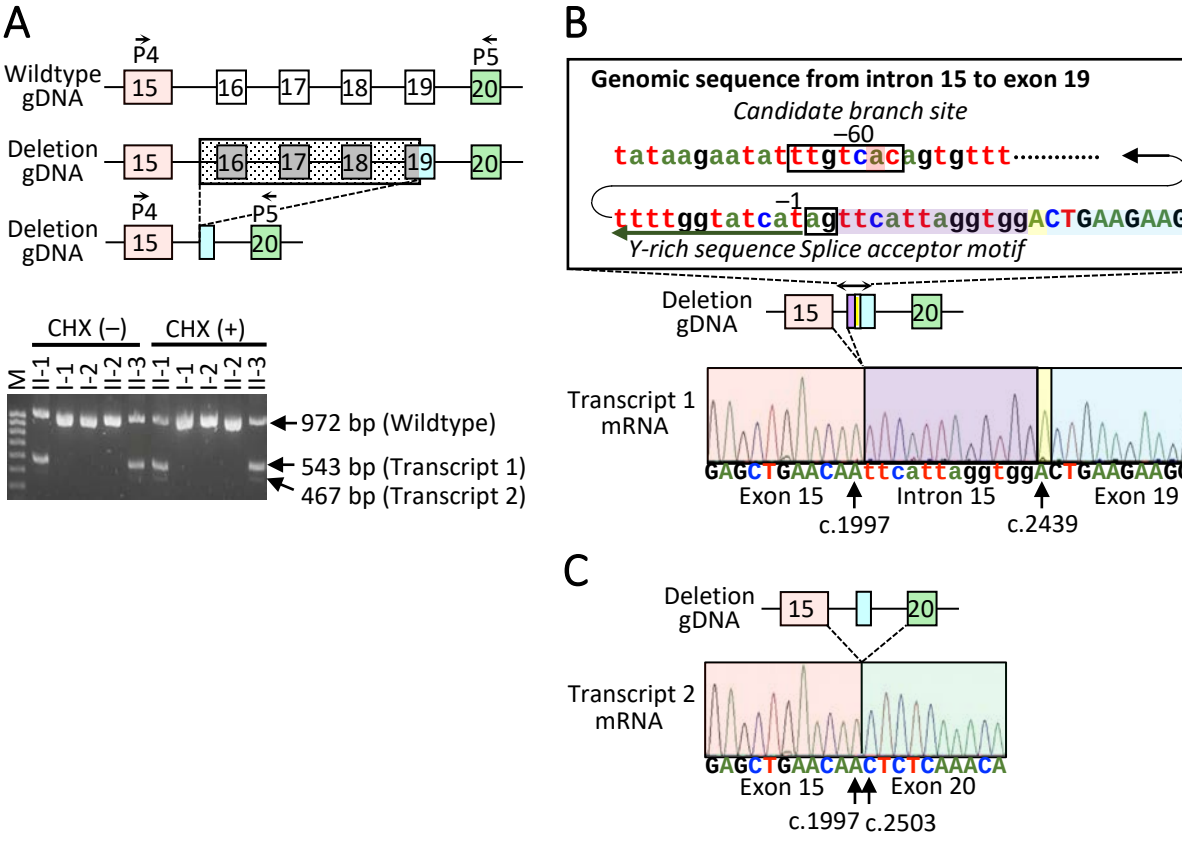
A
Wildtype gDNA
P4
P5
15
16
17
18
19
20
Deletion gDNA
Deletion gDNA
CHX (–)
CHX (+)
M
II-1
I-1
I-2
II-2
II-3
II-1
I-1
I-2
II-2
II-3
972 bp (Wildtype)
543 bp (Transcript 1)
467 bp (Transcript 2)
B
Genomic sequence from intron 15 to exon 19
Candidate branch site
–60
tataagaatatttgtcacagtgttt
–1
ttttggtatcatagttcattaggtggACTGAAGAAGGC
Y-rich sequence Splice acceptor motif
Deletion gDNA
Transcript 1 mRNA
GAGCTGAACAATtcattaggtggACTGAAGAAGGCC
Exon 15
Intron 15
Exon 19
c.1997
c.2439
C
Deletion gDNA
Transcript 2 mRNA
GAGCTGAACAACTCTCAAACA
Exon 15
Exon 20
c.1997
c.2503